Hydrol. Earth Syst. Sci. Discuss., 12, 975–1015, 2015
www.hydrol-earth-syst-sci-discuss.net/12/975/2015/
doi:10.5194/hessd-12-975-2015

Hydrology and Earth System Sciences
Open Access
Discussions

Understanding runoff processes in a semi-arid environment through isotope and hydrochemical hydrograph separations

V. V. Camacho[1], **A. M. L Saraiva Okello**[1,2], **J. W. Wenninger**[1,2], **and S. Uhlenbrook**[1,2]

[1]Department of Water Science and Engineering, UNESCO-IHE Institute for Water Education, P.O. Box 3015, 2601 DA Delft, the Netherlands
[2]Section of Water Resources, Delft University of Technology, P.O. Box 5048, 2600 GA Delft, the Netherlands

Received: 19 December 2014 – Accepted: 27 December 2014 – Published: 22 January 2015

Correspondence to: V. V. Camacho (viviancamacho@gmail.com)

Published by Copernicus Publications on behalf of the European Geosciences Union.

Abstract

The understanding of runoff generation mechanisms is crucial for the sustainable management of river basins such as the allocation of water resources or the prediction of floods and droughts. However, identifying the mechanisms of runoff generation has been a challenging task, even more so in arid and semi-arid areas where high rainfall and streamflow variability, high evaporation rates, and deep groundwater reservoirs increase the complexity of hydrological process dynamics. Isotope and hydrochemical tracers have proven to be useful in identifying runoff components and their characteristics. Moreover, although widely used in humid-temperate regions, isotope hydrograph separations have not been studied in detail in arid and semi-arid areas. Thus the purpose of this study is to determine if isotope hydrograph separations are suitable for the quantification and characterization of runoff components in a semi-arid catchment considering the hydrological complexities of these regions. Through a hydrochemical characterization of the surface water and groundwater sources of the catchment and two and three component hydrograph separations, runoff components of the Kaap Catchment in South Africa were quantified using both, isotope and hydrochemical tracers. No major disadvantages while using isotope tracers over hydrochemical tracers were found. Hydrograph separation results showed that runoff in the Kaap catchment is mainly generated by groundwater sources. Two-component hydrograph separations revealed groundwater contributions between 64 and 98 % of total runoff. By means of three-component hydrograph separations, runoff components were further separated into direct runoff, shallow and deep groundwater components. Direct runoff, defined as the direct precipitation on the stream channel and overland flow, contributed up to 41 % of total runoff during wet catchment conditions. Shallow groundwater defined as the soil water and near-surface water component, contributed up to 45 % of total runoff, and deep groundwater contributed up to 84 % of total runoff. A strong correlation for the four studied events was found between the antecedent precipitation conditions and direct runoff. These findings suggest that direct runoff is enhanced by wetter condi-

HESSD
12, 975–1015, 2015

tions in the catchment which trigger saturation excess overland flow as observed in the hydrograph separations.

1 Introduction

Understanding runoff processes facilitates the evaluation of surface water and groundwater risks with respect to quality and quantity (Uhlenbrook et al., 2002). It assists in quantifying water resources for water allocation, hydropower production, design of hydraulic structures, environmental flows, drought and flood management, and water quality purposes (Blöschl et al., 2013). The need for understanding runoff processes has led to the development of tools such as hydrograph separation techniques that identify runoff components in stream water, flowpaths, residence times and contributions to total runoff (Klaus and McDonnell, 2013; Hrachowitz et al., 2009; Weiler et al., 2003). Several hydrograph separation studies using environmental isotopes and geochemical tracers have been carried out in forested, semi-humid environments which have led to new insights of runoff processes in these areas (e.g. Pearce et al., 1986; Bazemore et al., 1994; Tetzlaff and Soulsby, 2008; Uhlenbrook et al., 2002; Burns et al., 2001). But, there is still a need for understanding runoff generation mechanisms in tropical, arid and semi-arid areas as they were much less investigated (Burns, 2002).

Studying runoff processes in arid and semi-arid regions has been challenging due to the high temporal and spatial variability of rainfall, high evaporation rates, sparse vegetation, deep groundwater resources, poorly developed soils, and in some cases the lack of surface runoff (Kendall and McDonnell, 1998; Blöschl et al., 2013; Hrachowitz et al., 2011; Wheater et al., 2008). In addition, the remoteness of some of these areas and financial constraints, as many semi-arid areas are located in developing countries has added extra difficulties for studying these regions. Precipitation in arid regions is characterized by its sporadic, high energy, and low frequency occurrence (Camarasa-Belmonte and Soriano, 2014; Kendall and McDonnell, 1998; Wheater et al., 2008). Dry spells can last for years, and rain events may vary from a few millimeters to hun-

HESSD
12, 975–1015, 2015

dreds of millimeters per year. These high intensity storms may generate most if not all the season's runoff (Love et al., 2010). The high intensity events can also increase erosion, thus reducing the soil infiltration capacity and enhancing the surface runoff component (Camarasa-Belmonte and Soriano, 2014). On the contrary, the lack of precipitation may also result in reduced to non-existent groundwater recharge (Kendall and McDonnell, 1998). In contrast to humid regions where evaporation is generally limited by the amount of energy available, evaporation in arid and semi-arid areas is usually limited by the water availability in the catchment (Wang et al., 2013). Thus evaporation becomes the dominant factor in driving the hydrology of arid and semi-arid areas (Kendall and McDonnell, 1998). Understanding the impact of evaporation on stream runoff processes becomes more complex due to the sparse nature of vegetation. An increase in vegetation due to a wetter rainfall season may result in higher evaporation rates, reduced streamflow and an increase in soil infiltration capacity (Hughes et al., 2007; Mostert et al., 1993). Other transmission losses such as infiltration through the stream channel bed may also reduce the total surface runoff volume generated. These losses are important for groundwater recharge as observed in south-west Saudi-Arabia where infiltration through the channel bed has been identified as the dominant groundwater recharge mechanism (Wheater et al., 2008; Costa et al., 2012).

This paper explores the runoff processes, including surface-groundwater interactions in the Kaap Catchment, South Africa by first studying the spatial hydrochemical characterization of the catchment and then, by separating the runoff components through isotope and geochemical tracer analysis. Moreover, the purpose of this paper is to determine the suitability of isotopic tracers for the characterization of runoff components in the Kaap catchment. Isotopes have proven to reveal runoff components and their characteristics in humid-temperate regions. However, the question of their applicability in the complex hydrology of arid and semi-arid regions still remains (Munyaneza et al., 2012; Hrachowitz et al., 2011; Zarei et al., 2014). Although analytical methods for hydrograph separation have been carried out in the the Kaap River, no accurate estimations of runoff components were retrieved in the area. Thus, this paper not only

HESSD
12, 975–1015, 2015

contributes to the understanding of runoff processes in semi-arid areas using environmental isotopes, but also provides a baseline for understanding surface and groundwater dynamics in the Incomati trans-boundary River system. The Kaap River is a major contributor of flow to the Crocodile River which flows into the Incomati trans-boundary River. The Incomati waters are shared by South Africa, Swaziland and Mozambique where tensions related to the management of water resources have led to the development of water-sharing agreements such as the Tripartite Interim Agreement on Water Sharing of the Maputo and Incomati Rivers (Van der Zaag and Carmo Vaz, 2003). The need for reliable data and understanding of the hydrological functioning of the system has been highlighted in these agreements (Slinger et al., 2010). In addition, the Kaap River and the neighboring catchments have experienced devastating floods in February 2000 and March 2014 with return periods exceeding 200 years (Smithers et al., 2001).

2 Study area

The Kaap catchment is located in the northeast of South Africa in the Mpumalanga province and has an area of approximately 1640 km^2 (Fig. 1). Nelspruit, the provincial capital, and Barberton are the closest urban areas to the Kaap with populations of approximately 125 000 and 35 000 inhabitants, respectively (GRIP, 2012). The study area is predominantly located in the Lowveld region with elevations ranging from 300 to 1800 m a.s.l. The average slope is 18 %.

The geology dates back to Archean times. Biotite granite is the predominant formation in the valley (Fig. 2c). Headwater streams originate on the weathered granite, which felsic properties indicate high concentrations of dissolved silica. Surrounding granite, lava formations or Onverwacht formations contain basaltic and peridotitic komatiite, which are low in silicates and high in magnesium. The Onverwatch formation is one of the oldest formations in the area. Formed in an ocean, it is rich in quartz, volcanic rocks and chert horizons (de Wit et al., 2011). Sandstones and shales are found

HESSD
12, 975–1015, 2015

in closer proximity to the Kaap River and at the Southern section of the catchment. In addition to the gneiss formation observed near the outlet, other formations include ultramafic (high in iron and low in silicates) rocks, quartzite and dolomite (Sharpe et al., 1986). Borehole logs near the upper Suidkaap and Noordkaap tributaries displayed a top layer of weathered granite (approximately 25 to 37 m in depth) followed by a thinner, less fractured granite layer and hard rock granite. Borehole logs analyzed in closer proximity to the catchment outlet presented more diverse formations including layers of clay, sand, greywacke and weathered shale.

Bushvelds and grasslands are the predominant land use in the Kaap Valley covering up to 68 % of the catchment (Fig. 2b). In the upstream region (western part of the catchment), approximately 25 % of the total catchment consists of pine and eucalyptus plantations used for paper and timber production. Sugar cane, citrus trees, and other cash crops are found in the downstream region where many diversion channels for irrigation are present. Irrigation demand in the Kaap catchment is approximately 56 mm a^{-1} (Mallory and Beater, 2009).

The climate is semi-arid with cool dry winters and hot wet summers. Between 2001 and 2012, recorded minimum and maximum daily air temperatures at the Barberton meteorological station ranged from 3 to 42 °C, with a long-term average of 20 °C (SASRI, 2013). The wet season lasts typically from October to March. Precipitation ranges from 583 to 1243 mm a^{-1} (WRC, 2005) with an average annual precipitation of 742 mm a^{-1}, and mean annual runoff coefficient of 0.14. The mean potential evaporation collected from Class A evaporation pan from SASRI and DWA stations (2002 to 2012) is 1014 mm a^{-1}.

The Kaap catchment contains three main tributaries; the Queens, the Upper Suidkaap and the Noordkaap. The highest monthly average flow during the year occurs in February with an average of 9.2 $m^3 s^{-1}$. The lowest monthly flow during the year occurs at the end of the dry season in September, reaching an average of 0.8 $m^3 s^{-1}$. Minimum and maximum daily average flows recorded between 1961 and 2012 at the Kaap outlet

HESSD
12, 975–1015, 2015

range from 0 to 483 $m^3 s^{-1}$. The long term mean flow at the outlet is 3.7 $m^3 s^{-1}$, which is equivalent to 55 mm a^{-1}.

3 Data and methods

3.1 Long-term datasets

Hydrological data in the catchment, including precipitation, evaporation, streamflow and groundwater records, were collected from the Department of Water Affairs (DWA), the South African Weather Service (SAWS), the South African Sugarcane Research Institute (SASRI), and the firm In-Situ Groundwater Consulting. Geological, topographical and land use GIS (Geographic Information Systems) data were obtained from the Water Research Commission 2005 study (WRC, 2005).

The average catchment precipitation was obtained by studying seven weather stations with daily rainfall data from 2001 to 2012. Only four stations were selected based on data availability and proximity to the catchment. These stations were X1E006, X1E007, Barberton and Malelane (Fig. 1). Missing rainfall values for Barberton (2 %) and X1E007 (33 %) were estimated by regression analysis. Malelane and X1E006 did not contain missing data. Using a Thiessen polygon distribution, the average rainfall was calculated for the catchment.

Average actual evaporation was calculated from daily Class A pan evaporation values from the Barberton and Malelane stations and daily Class S pan evaporation from X1E006 and X1E007 stations from 2003 to 2012. Daily pan evaporation values were aggregated to monthly pan evaporation values. Class S pan evaporation was converted to Class A pan evaporation following the Water Resources of South Africa 1990 study WR90 (Midgley et al., 1994). Class A evaporation was converted to reference evaporation using the guidelines for crop water requirements (Allen et al., 1998) and reference evaporation was corrected for the specific land uses using data from the land satellite imagery collected from the Incomati Water Availability Assessment Study (Mallory

HESSD
12, 975–1015, 2015

and Beater, 2009). Using a long term water balance from 2003 to 2012, actual mean evaporation rates were found.

To analyze the stream flow response at the outlet and tributaries, daily discharges at X2H022 (Outlet), X2H008 (Queens), X2H031 and X2H024 (Suidkaap) and X2H010 (Noordkaap) stream gauges were obtained from the DWA. The locations of the stations are shown in Fig. 2a.

3.2 Field and laboratory methods

3.2.1 General

A field campaign from 20 November 2013 to 4 February 2014 was carried out to obtain an overview of the hydrochemistry of the catchment prior to the rainy season and to collect data for hydrograph separation studies.

Stream discharge collected from DWA data loggers (water levels converted to stream discharge using DWA rating curve) were retrieved at the outlet with a frequency of 12 min (0.2 h) from 30 October 2013 to 17 February 2014. Hourly precipitation rates were obtained from the Incomati Catchment Management Agency (ICMA) rain gauges at Roffiekultuur, Nelshoogte Bos, Satico, and Josefdal Boarder from 1 October 2013 to 28 February 2014 (see locations on Fig. 2a).

3.2.2 Water samples

Water samples were collected from the tributaries, main river, one spring, and two drinking water wells as shown in Fig. 2a. Each location was sampled twice during dry weather conditions. Each sample of approximately 250 mL was collected in polyethylene bottles, rinsed three times before the final sample was taken to avoid contamination, and refrigerated for sample preservation. Electrical conductivity (EC), pH and temperature were measured in-situ using a WTW conductivity meter.

HESSD
12, 975–1015, 2015

3.2.3 Rain sampling

To obtain the isotopic and hydrochemical reference of rainfall, bulk rain samples were collected in the upstream and downstream part of the catchment. The rain samplers were constructed according to standards of the International Atomic Energy Agency (IAEA) to avoid re-evaporation (Gröning et al., 2012). The upstream rain samples average had a more depleted isotopic signature (−5.1 ‰ for δ^{18}O; −30.2 ‰ for δ^{2}H) than the lower elevation rain samples average (−4.4 ‰ for δ^{18}O; −24.7 ‰ for δ^{2}H). Thus an average of upstream and downstream samples per rain event was used for the rainfall end member concentrations for each hydrograph separation.

Rainfall characteristics, including duration, total rain amount, maximum and average intensity, and antecedent precipitation index were estimated for each rain event. A rainfall event was defined as a rainfall occurrence with rainfall intensity greater than 1 mm h^{-1}, and intermittence less than four hours as observed in a similar study in a semi-arid area by Wenninger et al. (2008). The Antecedent Precipitation Index (API) for n days prior the event were calculated using Eq. (1):

$$\mathrm{API}_{-n} = \sum_{i=1}^{7} P_{(-n-1+i)}(0.1i) \quad (1)$$

where P in (mm h^{-1}) stands for precipitation and i is number corresponding to the day of rainfall. For this study, API indexes were calculated for the seven, fourteen and thirty days prior to the event. Peak flow, runoff depth, and time to peak were determined for each event.

3.2.4 Automatic sampler

During the rainy season 2013–2014, four events that occurred on 12–13 December (Event 1), 28–30 December (Event 2), 13 January (Event 3) and 30–31 January (Event 4) were sampled using an automatic sampler manufactured by the University of

HESSD
12, 975–1015, 2015

KwaZulu-Natal (UKZN). The first two events were sampled on a volume basis obtaining 22 samples for Event 1, and 5 samples for Event 2 (a smaller number of samples were obtained for Event 2 due to photo sensor failure in the automatic sampler). Events 3 and 4 were sampled using a time based strategy obtaining 13 samples for Event 3, and 36 samples for Event 4. A total volume of approximately 100 mL was obtained for each sample.

3.2.5 Chemical analysis of water samples

All samples were refrigerated, filtered, and analyzed for HCO_3 and Cl using a Hach Digital Titrator, and SiO_2 using a Hach DR890 Portable colorimeter within 48 h. Then, samples were transported to the UNESCO-IHE laboratory in the Netherlands for further chemical analysis. The samples were analyzed for major anions, cations and stable isotopes as listed in Table 1.

3.3 Data analysis

3.3.1 Groundwater analysis

Groundwater chemical data for 240 boreholes and 18 borehole logs were obtained from In-Situ Groundwater Consultants covering the different geological formations (granite, lava, arenite, and gneiss). For 27 out of the 240 boreholes, pH, $CaCO_3$, Mg, Ca, Na, K, Cl, NO_3-N, F, SO_4, SiO_2, Al, Fe, and Mn data were available. The remaining boreholes had only information on EC, static water table depth, and physical characteristics of the borehole.

Borehole chemical data was classified according to the geological formations. The classified data distribution was observed using GIS, and basic statistical analysis was carried out to determine the control of geology over the hydrochemistry of groundwater.

HESSD
12, 975–1015, 2015

To gain better insights with regard to groundwater flow, groundwater contour lines were created using an Inversed Distance Weighted (IDW) interpolation of the static water tables from the boreholes.

3.3.2 End Member Mixing Analysis (EMMA)

Suitable parameters for hydrograph separation were identified by creating mixing diagrams of EC ($\mu S\,cm^{-1}$), SiO_2, $CaCO_3$, Cl, SO_4, Na, Mg, K, Ca (in mgL^{-1}) and δ^2H and $\delta^{18}O$ (‰ VSMOW). A principal component analysis was carried out based on the method described by Christophersen and Hooper (1992). Only not statistical correlated parameters were used. From these, the possibility of three end members was explored. In addition, parameters were plotted against discharge to observe dilution and hysteresis effects.

3.3.3 Hydrograph separation

Isotope and hydrochemical data were combined with discharge data to perform a multi-component hydrograph separation based on steady state mass balance equations as described, for instance, in Uhlenbrook et al. (2002). The number of tracers ($n-1$) was dependent on the number of runoff components (n). Equations (3) and (4) were applied in dividing the total runoff, Q_T, into two and three runoff components.

$$Q_T = Q_1 + Q_2 \ldots + Q_n \quad (2)$$

$$c_T Q_T = c_1 Q_1 + c_2 Q_2 \ldots + c_n Q_n \quad (3)$$

Where Q_1, Q_2 and Q_n are the runoff components in $m^3\,s^{-1}$ and c_T, c_1, c_2 and c_n are the concentrations of total runoff, and runoff components.

HESSD
12, 975–1015, 2015

3.3.4 Uncertainty estimation

Uhlenbrook and Hoeg (2003) showed that during the quantification of runoff components, uncertainties due to tracer and analytical measurements, intra-storm variability, elevation and temperature, solution of minerals, and the spatial heterogeneity of the parameter concentrations occur. For the Kaap river hydrograph separations, these uncertainties were accounted by the spatial hydrochemical characterization of the catchment and by sampling rainfall during each event and at different locations. Moreover, tracer end-members and analytical uncertainties were estimated using a Gaussian error propagation technique and a confidence interval of 70 % as described by Genereux (1998) and Liu et al. (2004).

$$W = \left\{ \left[\frac{\partial y}{\partial x_1} W_{x1} \right]^2 + \left[\frac{\partial y}{\partial x_2} W_{x2} \right]^2 + \ldots + \left[\frac{\partial y}{\partial x_n} W_{\mathrm{xs}} \right]^2 \right\}^{\frac{1}{2}} \quad (4)$$

W is the estimated uncertainty of each runoff component (e.g. direct runoff, shallow and deep groundwater components). W_{x1}, and W_{x2}, are the SD of the end-members. W_{xs} is the analytical uncertainty and the partial derivatives $\frac{\partial y}{\partial x_1}$, $\frac{\partial y}{\partial x_2}$ and $\frac{\partial y}{\partial x_n}$ are the uncertainties of the runoff component contributions with respect to the tracer concentrations.

4 Results

4.1 Hydrogeochemistry and groundwater flow

The variability of the catchment's groundwater quality parameters was studied from borehole data. Electrical conductivities in the granite region had the lowest electrical conductivity (EC) values (average 383 $\mu S\,cm^{-1}$), while the gneiss formation, near the outlet, had the largest EC average of 1140 $\mu S\,cm^{-1}$. Lava and arenite formations had

HESSD
12, 975–1015, 2015

mean EC values of 938 and 525 µS cm^{-1}, respectively. The gneiss and lava formations had higher concentration averages of chloride and calcium carbonate than the granite and arenite formations. These can be seen in the box plots in Fig. 3.

Groundwater contour lines followed the topographical relief. The highest water tables were observed at the north boundary of the catchment with water tables up to 1150 m (Fig. 2d). From the groundwater contour map, it was observed that groundwater moves toward the stream indicating a gaining river system. Time series from boreholes showed not a significant change in water tables due to seasonal or long-term changes.

4.2 Baseflow and spatial hydrochemical characterization

Baseflow at the catchment outlet (X2H022) was characterized by analyzing DWA long-term water quality data and by field sampling prior to the rainy season 2013–2014. Results from the field sampling are shown in Table 2.

The upper section of the catchment, mainly dominated by granite, is characterized by low to moderate electrical conductivities. Long-term mean electrical conductivities (sampled monthly by the DWA from 1984 to 2012) for the Upper Suidkaap and Noordkaap tributaries were 75 and 104 µS cm^{-1}, respectively. On the contrary, the catchment outlet had a higher long-term average EC of 572 µS cm^{-1} (DWA long-term monthly average from 1977 to 2012).

4.3 Rainfall–runoff observations

Table 3 summarizes the rainfall–runoff observations for the four studied events. The events had distinctive characteristics showing large variability in peak flows, Antecedent Precipitation Index (API), rainfall duration, rain depth and maximum and average intensities. Event 1 had the highest peak flow at 124 m^3 s^{-1} while Event 3 had the smallest peak flow at 6.5 m^3 s^{-1}. API indices, especially API$_{-7}$, differed from very wet conditions during Event 1 (39 mm) to very dry conditions (1 mm) during Event 2. Event 1 was a relatively short event (7 h) with high antecedent precipitation conditions and

HESSD
12, 975–1015, 2015

high rain intensities generating the largest amount of runoff at the outlet. In contrast, Event 3 was a short event with average rain intensity that generated the lowest peak flow.

4.4 Response of isotopes and hydrochemical parameters

During the storm events, most hydrochemical parameters (EC, Ca, Mg, Na, SiO_2 and Cl) and water isotopes (δ^2H and $\delta^{18}O$) showed dilution responses except for potassium (Fig. 4). During Event 1, EC's initial value of 317 µS cm^{-1} decreased to 247 µS cm^{-1} during peak flow. Similarly, $CaCO_3$ and SiO_2 decreased from 115 to 82 mg L^{-1}, and 21.1 to 19.6 mg L^{-1}, respectively. $\delta^{18}O$ (−2.9 ‰) and δ^2H (−7.0 ‰) decreased to −3.2 ‰ and −12.6 ‰, respectively. Potassium concentrations increased from 1.3 to 2.8 mg L^{-1}. For Event 2, a smaller number of samples were collected due to malfunctions of the automatic sampler. However, dilution of SiO_2 and Cl, and an increase in potassium concentrations were observed. Event 3 and 4 were smaller events, but a smaller sampling interval showed the same dilution behavior of the sampled parameters and the increase in potassium concentrations.

4.5 Two-component hydrograph separation

Event and pre-event components were separated using $\delta^{18}O$ and δ^2H, and direct runoff and groundwater were separated using EC, SiO_2, $CaCO_3$, and Mg. For simplicity, the two component hydrograph separation components in this study are referred as direct runoff and groundwater components. Direct runoff was considered the portion of runoff from event water and was characterized using the rain samples collected upstream and downstream inside the catchment. Groundwater end members were obtained from the initial stream water samples before the rainfall started. Events 1 and 4 had the largest contributions of direct runoff among the four events accounting for 29 % in case of Event 1 and up to 36 % for Event 4 (Table 4). Events 2 and 3 had lower

HESSD
12, 975–1015, 2015

direct runoff contributions ranging from 5 to 13 % for Event 2 and 2 to 12 % for Event 3. Figure 5 presents the two component hydrograph separations for the four events.

4.6 Isotope hydrograph separation vs. hydrochemical hydrograph separation

Hydrochemical tracers usually separate direct runoff from groundwater sources while isotopes separate old water from new water. A comparison between "old" and "groundwater" components obtained during the four events was carried out to investigate to what extend these components are similar. This allowed us to determine the suitability of isotopic hydrograph separations vs. hydrochemical separations for semi-arid environments. Figure 6 present the percentages of groundwater and old water contributions using environmental isotopes (δ^2H and δ^{18}O) and hydrochemical (EC, SiO_2, $CaCO_3$ and Mg) tracers for the four investigated events. It is noted that Events 1 and 4 have smaller contributions of groundwater than Events 3 and 4. Two instances (one for Event 4 and one for Event 2) show that old water resembles groundwater. The data points above the line present instances where old water is not necessarily groundwater but water stored before the event. No major differences are observed from old water and groundwater contributions, indicating that isotope tracers are suitable for the hydrograph separations in the Kaap River catchment.

4.7 End Member Mixing Analysis (EMMA)

To further differentiate the runoff components, a Principal Component Analysis (PCA) was carried out on twelve solutes (EC, SiO_2, $CaCO_3$, Cl, NO_3-N, SO_4, Na, Mg, K, Ca, δ^{18}O and δ^2H) using the statistical software R. The correlation matrix was used for the PCA. Results indicated that 90 % of the variability is explained by two principal components (m). Thus, the number of end-members (n) can be chosen as ($n = m+1$) leading to a three component hydrograph separation (Christophersen and Hooper, 1992). Figure 7 shows the biplot of principal components where the orthogonal vectors indicate no dependency between parameters. This is observed for δ^{18}O, δ^2H, K, and NO_3.

HESSD
12, 975–1015, 2015

The clustering of the hydrochemical parameters reveals the strong correlation between these parameters (SiO_2, $CaCO_3$, Ca, EC, Mg, Na, Cl, and SO_4). Potassium shows a negative strong correlation with the clustered parameters but not with the water isotopes and NO_3. Thus for the three component hydrograph separations, orthogonal vectors with weak Pearson correlations were selected. These are K and $\delta^{18}O$ ($r = -0.28$) and K and $\delta^{2}H$ ($r = 0.45$). Nitrate was not selected due to its non-conservative properties. Potassium was identified as a useful tracer due to its increasing concentrations during runoff peaks. This high potassium concentration suggested the presence of soil water influenced by vegetation. Furthermore, to account for additional near surface water, this component is referred as the shallow groundwater component during this study.

The mixing plot for $\delta^{2}H$ and K is presented in Fig. 8. The direct runoff end member was characterized by the upstream and downstream rain samples. These had a low K average (0.5 mg L^{-1}) and depleted $\delta^{18}O$ and $\delta^{2}H$ values (−4.8 ‰ for $\delta^{18}O$; −27.5 ‰ for $\delta^{2}H$). A spring sample was used to characterize the deep groundwater component which contained more enriched $\delta^{18}O$ and $\delta^{2}H$ values (−0.9 ‰ for $\delta^{18}O$; −2.2 ‰ for $\delta^{2}H$) and low K concentration (0.7 mg L^{-1}). The shallow groundwater end member was estimated considering the high K concentrations (4 mg L^{-1}) and slightly less depleted $\delta^{18}O$ and $\delta^{2}H$ (−3.5 ‰ for $\delta^{18}O$; −7.0 ‰ for $\delta^{2}H$) observed in the stream samples. The error bars in Fig. 8 were found from the SD for the rain samples. For the shallow and deep groundwater components, an interval of ±10 % of the end-member was used to plot the error bars for these components.

4.8 Three-component hydrograph separation

Direct runoff contributions obtained during the 3-component hydrograph separations (Table 5 and Fig. 9) concur with the 2-component hydrograph separations. Events 1 and 4 were characterized by higher contributions of direct runoff than Events 2 and 3. Moreover, Event 1 also had a higher contribution of shallow groundwater that peaked during the total runoff peak. Events 2, 3 and 4 had higher deep groundwater con-

HESSD
12, 975–1015, 2015

tributions. Uncertainties for the 3-component hydrograph separations can be seen in Table 5.

5 Discussion

5.1 Runoff processes in the Kaap catchment

From the mixing diagrams, groundwater analysis and spatial characterization of the catchment, the runoff components were identified and characterized (Table 6 and Fig. 10). The groundwater analysis suggested two sources of groundwater of different ionic content at the upper and lower sections of the catchment. In the upstream area, granite is the dominant formation explaining the lower ionic content in groundwater in contrast to the downstream areas where geologically diverse formations and land use increase the ionic content of groundwater. The weathered granite layer allows rain to infiltrate to the deeper groundwater reservoir (GW_D) through preferential flow paths with less contact time for weathering processes to occur. This explains the hydrochemical signature of the deep groundwater component, which is characterized by its moderate electrical conductivities, moderate to high dissolved silica, lower ionic content and low potassium concentrations. The chemical signature of the shallow groundwater component (GW_S) is characterized by the high electrical conductivities, alkalinity, sulphates, potassium, and nitrates which are washed from top geological layers with large ionic content and land uses such as agriculture and mining which are more predominant in the downstream region of the catchment.

Groundwater–surface water interactions studies (Petersen, 2012) in the nearby Kruger National Park (KNP) have shown that groundwater recharge occurs mostly during the wet season and groundwater flow travels in accordance with the topographical relief. Petersen (2012) studied the dominant flow mechanisms in KNP comparing two geographic areas: a granite dominated area in the west and a basaltic rock dominated area in the east. The granite section (approximately 30 km east from the Kaap out-

HESSD
12, 975–1015, 2015

let) was mainly characterized by the steep topography which favors overland flow to infiltrate through depressions, cracks and fractures by preferential pathways while the south basaltic section presents a flatter topography allowing piston flow processes to be more predominant. Petersen (2012) identified the type of aquifers found within KNP. These include: alluvial aquifers along the river channels formed of granular material, composite aquifers of regolith overlaid by bedrock, and deep fractured aquifers of igneous or metamorphic rocks with complex interconnected fractures. Petersen (2012) findings, covering studies of approximately 1011 boreholes in KNP, support the findings in the Kaap catchment where high fracturing in the granite section allows recharge of deeper groundwater reservoirs through preferential flow paths.

5.2 Catchment's response dependency on antecedent precipitation

Hydrograph separation results showed that there is a direct runoff contribution (2–36 %) to total runoff during storm events for the Kaap River. Similar results have been obtained for other catchments in semi-arid areas. For instance, Hrachowitz et al. (2011) in their study in four nested catchments in Tanzania found direct runoff contributions of 9 %. Similarly, Munyaneza et al. (2012) found groundwater contributions up to 80 % of total runoff in the Mingina catchment in Rwanda during the two and three-hydrograph separations in a 258 km^2 catchment. The importance of sub-surface flow in semi-arid catchments is also illustrated in Wenninger et al. (2008) in the Weatherley catchment in the Eastern Cape in South Africa. Similarly, Zarei et al. (2014) showed that the event water contribution in a 283 km^2 catchment in a semi-arid area in Iran was directly affected by a wetting cycle contributing up to 10 % of total runoff.

From the several variables considered such as geology, topography and rainfall characteristics studied for the four events, the direct runoff component was most sensitive to the antecedent precipitation index. This is observed during Events 1 and 4 where API_{-7} values are the largest among the four events and direct runoff contributions are also the largest for these events. The relationship between API_{-7} and direct runoff generation is supported by a strong Pearson correlation (0.76–0.94). This suggests that

HESSD
12, 975–1015, 2015

direct runoff is enhanced by wetter conditions in the catchment due to saturation in the subsurface triggering saturation overland flow. The influence of antecedent moisture conditions is also noted in Hrachowitz et al. (2004) where the 5 day antecedent precipitation and soil moisture conditions were closely related to direct runoff generation. Similarly, Hrachowitz et al. (2011) observed that the differences in runoff generation from two sub-catchments (the Ndolwa and Vudee catchments) in Tanzania were due to differences in preceding wetness conditions.

5.3 Complexities of runoff processes understanding in semi-arid areas

The combination of climatic and hydrological processes influenced by topography, geology, soils and land use make catchments complex systems. Furthermore, catchments become more non-linear as aridity increases and runoff processes become more spatially and temporally heterogeneous than in humid regions (Blöschl et al., 2013; Farmer et al., 2003). Thus, understanding hydrological processes in arid catchments becomes more difficult due to high variability of rainfall and streamflow, high evaporation losses, long infiltration pathways, permeable stream channel beds and often deep groundwater reservoirs (Kendall and McDonnell, 1998; Hughes, 2007; Trambauer et al., 2013).

The high variability of rainfall enhances the difficulties of runoff prediction by triggering different runoff responses. For instance, high intensity storms tend to generate overland flow in the form of infiltration excess overland flow (Smith and Goodrich, 2005), while high antecedent precipitation conditions enhance saturation excess overland flow. This effect is visible in this study during Event 1 where the high antecedent precipitation index suggested saturation of the subsurface, thus reducing the infiltration capacity and enhancing saturation excess overland flow. The opposite is observed for Events 2 and 3 where the low soil moisture conditions allow more rainfall to infiltrate activating other runoff processes such as preferential vertical flow.

Although not included in this study, inter-annual variability, evaporation, hydraulic connectivity, sparse vegetation and interception have shown to change the behavior of runoff processes in arid and semi-arid areas. For instance, inter-annual rainfall vari-

HESSD
12, 975–1015, 2015

ability is closely related to high evaporation losses. Hughes (2007) illustrates this by presenting a study performed in a Namibian Basin by Mostert et al. (1993). This study found that during wetter seasons, vegetation cover and total evaporation increased thus reducing the amount of runoff reaching the outlet. Conversely, hydraulic connectivity in arid environments is limited by the reduced soil moisture conditions in these areas. This disconnection, often due to water as the limiting factor, is observed by the reduced groundwater availability. Arid and semi-arid areas hold approximately only 2 % of the global groundwater resources, while humid-temperate areas and equatorial-tropical areas cover the remaining global groundwater resources (Margat and van der Gun, 2013). This hydraulic disconnection causes longer flowpaths and may lead to reductions in streamflow (Moller et al., 2007).

Other fluxes such as interception and flow through permeable stream beds pose a greater challenge to the understanding runoff processes in semi-arid areas. Interception can further decrease the hydrologic connectivity in semi-arid environments breaking the link between meteoric water and groundwater. This is observed in the Zhulube catchment in Zimbabwe where interception accounted up to 56 % of rainfall during the dry season (Love et al., 2010). Similarly, transmission losses due to the high degree of fracturing of stream beds can significantly reduce streamflow but recharge groundwater systems. This effect is visible especially during rare but intense floods. Unfortunately, these losses have not been quantified yet, but are important factors for the accurate prediction of runoff (Hughes, 2007).

Thus, this study illustrated the effects of temporal rainfall variability during the wet season suggesting the influence of antecedent precipitation conditions on direct runoff generation. However, studying the effects of spatial and inter-annual rainfall variability, high evaporation, sparse vegetation and poorly developed soils, and deep groundwater resources on streamflow generation is still required for the better understanding of runoff processes in semi-arid areas.

HESSD
12, 975–1015, 2015

6 Conclusions

The Kaap catchment has suffered devastating floods that affect greatly the transboundary Incomati basin, in particular downstream areas in South Africa, Swaziland and Mozambique where recent floods have caused significant economic and social losses. Runoff processes were poorly understood in the Kaap catchment limiting rainfall–runoff models to lead to better informed water management decisions. Through hydrometric measurements, tracers and groundwater observations, runoff components and main runoff generation processes were identified and quantified in the Kaap catchment for the wet season 2013–2014. The suitability of isotope hydrograph separation was tested by comparing it to hydrochemical hydrograph separations showing no major differences between these tracers. Hydrograph separations showed that groundwater was the dominant runoff component for the wet season 2013–2014. Moreover, a strong correlation between direct runoff generation and antecedent precipitation conditions was found for the studied events. Direct runoff was enhanced by high antecedent precipitation activating saturation excess overland flow. Similar groundwater contributions have been observed in other studies in semi-arid areas (Wenninger et al., 2008; Hrachowitz et al., 2011; Munyaneza et al., 2012). Moreover, the understanding of runoff generation mechanisms in the Kaap catchment contributes to the limited number of hydrological processes studies and in particular hydrograph separation studies in semi-arid regions for the proper management of water resources.

Acknowledgements. This study was carried out under the umbrella of the RISK-based Operational water MANagement for the Incomati River basin (RISKOMAN) project. The authors would like to thank the RISKOMAN partners: UNESCO-IHE, Universidade Eduardo Mondlane (Mozambique), University of KwaZulu-Natal (South Africa), the Komati River Basin Authority (Swaziland) and Incomati Catchment Management Agency (South Africa) for their financial and technical cooperation. This research has also been supported by the International Foundation for Science (IFS) Stockholm, Sweden, through a grant (W/5340-1) to Aline M. L. Saraiva Okello. Gratitude is also expressed to Ilyas Masih (UNESCO-IHE), Thomas Gyedu Ababio (ICMA), Graham Jewitt (UKZN), Cobus Pretorius (UKZN), Eddie Riddell (SANParks), Gareth

HESSD
12, 975–1015, 2015

Bird (Independent), the ICMA staff, In-Situ Groundwater Consulting, IAEA, UNESCO-IHE laboratory staff and the advanced class program at UNESCO-IHE funded by UNEP-DHI.

References

Allen, R. G., Pereira, L. S., Raes, D., and Smith, M.: Crop evapotranspiration – Guidelines for computing crop water requirements – FAO Irrigation and drainage paper 56, Food and Agriculture Organization of the United Nations, Rome, 1998.

Bazemore, D. E., Eshleman, K. N., and Hollenbeck, K. J.: The role of soil-water in stormflow generation in a forested headwater catchment – synthesis of natural tracer and hydrometric evidence, J. Hydrol., 162, 47–75, doi:10.1016/0022-1694(94)90004-3, 1994.

Blöschl, G., Sivapalan, M., Wagener, T., Viglione, A., and Savenije, H.: Runoff Prediction in Ungauged Basins, Cambridge University Press, 2013.

Burns, D. A.: Stormflow-hydrograph separation based on isotopes: the thrill is gone – what's next?, Hydrol. Process., 16, 1515–1517, doi:10.1002/Hyp.5008, 2002.

Burns, D. A., McDonnell, J. J., Hooper, R. P., Peters, N. E., Freer, J. E., Kendall, C., and Beven, K.: Quantifying contributions to storm runoff through end-member mixing analysis and hydrologic measurements at the Panola Mountain Research Watershed (Georgia, USA), Hydrol. Process., 15, 1903–1924, doi:10.1002/Hyp.246, 2001.

Camarasa-Belmonte, A. M. and Soriano, J.: Empirical study of extreme rainfall intensity in a semi-arid environment at different time scales, J. Arid Environ., 100–101, 63–71, 2014.

Christophersen, N. and Hooper, R. P.: Multivariate-analysis of stream water chemical-data – the use of principal components-analysis for the end-member mixing problem, Water Resour. Res., 28, 99–107, doi:10.1029/91wr02518, 1992.

Costa, A. C., Bronstert, A., and de Araújo, J. C.: A channel transmission losses model for different dryland rivers, Hydrol. Earth Syst. Sci., 16, 1111–1135, doi:10.5194/hess-16-1111-2012, 2012.

de Wit, M. J., Furnes, H., and Robins, B.: Geology and tectonostratigraphy of the Onverwacht Suite, Barberton Greenstone Belt, South Africa, Precambrian Res., 168, 1–27, 2011.

Farmer, D., Sivapalan, M., and Jothityangkoon, C.: Climate, soil, and vegetation controls upon the variability of water balance in temperate and semiarid landscapes: downward approach to water balance analysis, Water Resour. Res., 39, 1035, doi:10.1029/2001WR000328, 2003.

HESSD
12, 975–1015, 2015

Genereux, D.: Quantifying uncertainty in tracer-based hydrograph separations, Water Resour. Res., 34, 915–919, doi:10.1029/98wr00010, 1998.
GRIP: Groundwater Resources Information Programme, Polokwane, South Africa, 2012.
Gröning, M., Lutz, H. O., Roller-Lutz, Z., Kralik, M., Gourcy, L., and Pöltenstein, L.: A simple rain collector preventing water re-evaporation dedicated for ^{18}O and δ^2H analysis of cumulative precipitation samples, J. Hydrol., 448–449, 195–200, 2012.
Hrachowitz, M., Soulsby, C., Tetzlaff, D., Dawson, J. J. C., Dunn, S. M., and Malcolm, I. A.: Using long-term data sets to understand transit times in contrasting headwater catchments, J. Hydrol., 367, 237–248, doi:10.1016/j.jhydrol.2009.01.001, 2009.
Hrachowitz, M., Bohte, R., Mul, M. L., Bogaard, T. A., Savenije, H. H. G., and Uhlenbrook, S.: On the value of combined event runoff and tracer analysis to improve understanding of catchment functioning in a data-scarce semi-arid area, Hydrol. Earth Syst. Sci., 15, 2007–2024, doi:10.5194/hess-15-2007-2011, 2011.
Hughes, D. A.: Modelling semi-arid and arid hydrology and water resources – the southern African experience, in: Hydrological Modelling in Arid and Semi-Arid Areas, Chap. 3, edited by: Wheater, H., Sorooshian, S., and Sharma, K. D., 29–40, Cambridge, Cambridge University Press, 2007.
Hughes, J. D., Khan, S., Crosbie, R. S., Helliwell, S., and Michalk, D. L.: Runoff and solute mobilization processes in a semiarid headwater catchment, Water Resour. Res., 43, W09402, doi:10.1029/2006WR005465, 2007.
Kendall, C. and McDonnell, J.: Isotope Tracers in Catchment Hydrology, Elsevier Science, Amsterdam, the Netherlands, 839 pp., 1998.
Klaus, J. and McDonnell, J. J.: Hydrograph separation using stable isotopes: review and evaluation, J. Hydrol., 505, 47–64, doi:10.1016/j.jhydrol.2013.09.006, 2013.
Liu, F. J., Williams, M. W., and Caine, N.: Source waters and flow paths in an alpine catchment, Colorado Front Range, United States, Water Resour. Res., 40, W09401, doi:10.1029/2004wr003076, 2004.
Love, D., Uhlenbrook, S., Corzo-Perez, G., Twomlow, S., and Zaag, P. v. d.: Rainfall–interception–evaporation–runoff relationships in a semi-arid catchment, northern Limpopo basin, Zimbabwe, Hydrolog. Sci. J., 55, 687–703, 2010.
Mallory, S. and Beater, A.: Inkomati Water Availability Assessment Study (IWAAS), Department of Water Affairs and Forestry (DWAF), Pretoria, 2009.

HESSD
12, 975–1015, 2015

Margat, J. and van der Gun, J.: Groundwater around the world, A Geographic Synopsis, edited by: Group, T. F., CRC Press/Balkema, Leiden, the Netherlands, 2013.
Midgley, D. C., Pittman, W. V., and Middleton, B. J.: Surface Water Resources of South Africa 1990, Report No. 298/1/94, Water Research Commission Pretoria, South Africa, 1994.
Mostert, A., McKenzie, R., and Crerar, S.: A rainfall/runoff model for ephemeral rivers in an arid or semi-arid environment, 6th South African National Hydrology Symposium, Pietermaritzburg, 219–224, 8–10 September, 1993.
Munyaneza, O., Wenninger, J., and Uhlenbrook, S.: Identification of runoff generation processes using hydrometric and tracer methods in a meso-scale catchment in Rwanda, Hydrol. Earth Syst. Sci., 16, 1991–2004, doi:10.5194/hess-16-1991-2012, 2012.
Pearce, A. J., Stewart, M. K., and Sklash, M. G.: Storm runoff generation in humid headwater catchments 1. Where does the water come from?, Water Resour. Res., 22, 1263–1272, 1986.
Petersen, R.: A conceptual understanding of groundwater recharge processes and surface-groundwater interactions in the Kruger National Park, Master in the Faculty of Natural Sciences, Department of Earth Sciences, University of the Western Cape, Bellville, 2012.
Sharpe, M. R., Sohnge, A. P., Zyl, J. S. v., Joubert, D. K., Mulder, M. P., Clubley-Armstrong, A. R., Plessis, C. P. d., Eeden, O. R. v., Rossouw, P. J., Visser, D. J. L., Viljoen, M. J., and Taljaard, J. J.: 2530 Barberton, Department of Minerals and Energy Affairs, Government Printer, South Africa, 1986.
Slinger, J. H., Hilders, M., and Dinis, J.: The practice of transboundary decision making on the Incomati River, Ecol. Soc., 15, 2010.
Smith, R. E. and Goodrich, D. C.: Rainfall excess overland flow, in: Encyclopedia of Hydrological Sciences, edited by: Anderson, M. G., John Wiley & Sons Ltd, 1707–1718, London, UK, 2005.
Smithers, J., Schulze, R., Pike, A., and Jewitt, G.: A hydrological perspective of the February 2000 floods: a case study in the Sabie River Catchment, Water SA, 27, 325–332, doi:10.4314/wsa.v27i3.4975, 2001.
Tetzlaff, D. and Soulsby, C.: Sources of baseflow in larger catchments – using tracers to develop a holistic understanding of runoff generation, J. Hydrol., 359, 287–302, doi:10.1016/j.jhydrol.2008.07.008, 2008.

HESSD
12, 975–1015, 2015

The South African Sugarcane Research Institute: available at: http://portal.sasa.org.za/weatherweb/weatherweb.ww_menus.menu_frame?menuid=1 (last access: 1 October 2013), 2013.
Trambauer, P., Maskey, S., Winsemius, H., Werner, M., and Uhlenbrook, S.: A review of continental scale hydrological models and their suitability for drought forecasting in (sub-Saharan) Africa, Phys. Chem. Earth, 66, 16–26, 2013.
Uhlenbrook, S. and Hoeg, S.: Quantifying uncertainties in tracer-based hydrograph separations: a case study for two-, three- and five-component hydrograph separations in a mountainous catchment, Hydrol. Process., 17, 431–453, doi:10.1002/Hyp.1134, 2003.
Uhlenbrook, S., Frey, M., Leibundgut, C., and Maloszewski, P.: Hydrograph separations in a mesoscale mountainous basin at event and seasonal timescales, Water Resour. Res., 38, 311–314, doi:10.1029/2001WR000938, 2002
Van der Zaag, P. and Carmo Vaz, A.: Sharing the Incomati water: cooperation and competition in the balance, Water Policy, 5, 346–368, 2003.
Wang, R., Kumar, M., and Marks, D.: Anomalous trend in soil evaporation in a semi-arid, snow-dominated watershed, Adv. Water Resour., 57, 32–40, 2013.
Weiler, M., McGlynn, B. L., McGuire, K. J., and McDonnell, J. J.: How does rainfall become runoff? A combined tracer and runoff transfer function approach, Water Resour. Res., 39, 1315 pp., doi:10.1029/2003WR002331, 2003.
Wenninger, J., Uhlenbrook, S., Lorentz, S., and Leibundgut, C.: Identification of runoff generation processes using combined hydrometric, tracer and geophysical methods in a headwater catchment in South Africa, Hydrolog. Sci. J., 53, 65–80, 2008.
Wheater, H., Sorooshian, S., and Sharma, K. D.: Hydrological Modelling in Arid and Semi-Arid Areas, University Press, Cambridge, UK, 195 pp., 2008.
WRC: Water resources of South Africa, 2005 study (WR2005), TT381, Pretoria, 2005.
Zarei, H., Akhondali, A. M., Mohammadzadeh, H., Radmanesh, F., and Laudon, H.: Runoff generation processes during the wet-up phase in a semi-arid basin in Iran, Hydrol. Earth Syst. Sci. Discuss., 11, 3787–3810, doi:10.5194/hessd-11-3787-2014, 2014.

HESSD
12, 975–1015, 2015

Table 1. UNESCO-IHE laboratory equipment used in chemical analysis of Kaap catchment samples.

	Parameter(s) analyzed	Equipment	Number of samples	Preservation method	Analytical uncertainty (σ)
Environmental Isotopes	^{18}O, ^{2}H	Isotope Analyzer LRG DLT-100	116	None	±0.2, ±1.5 (‰)
Cations	Ca^{2+}, Mg^{2+}, Na^{+}, K^{+}	Thermo Fisher Scientific XSeries 2 ICP-MS	116	Nitric acid (HNO_3)	±0.2 ($mg\,L^{-1}$)
Anions	Cl^{-}, NO_3^{-}-N, SO_4^{2-}, PO_4^{3-}	Dionex ICS-1000	116	Refrigerated at $< 4\,^{\circ}C$	±0.2 ($mg\,L^{-1}$)

HESSD
12, 975–1015, 2015

Table 2. List of mean values of hydrochemical parameters obtained during field campaign 2013–2014.

Parameter	Location Suidkaap	Queens	Noordkaap	Outlet
EC ($\mu S\,cm^{-1}$)	84.0	128.7	92.9	443.0
SiO_2 ($mg\,L^{-1}$)	22.4	17.0	20.9	24.1
$CaCO_3$ ($mg\,L^{-1}$)	38.5	59.5	41.3	154.0
Cl ($mg\,L^{-1}$)	3.8	3.6	2.8	15.5
SO_4 ($mg\,L^{-1}$)	1.8	4.1	1.6	47.2
Na ($mg\,L^{-1}$)	7.5	7.1	7.3	29.3
Mg ($mg\,L^{-1}$)	2.8	7.4	3.7	25.3
Ca ($mg\,L^{-1}$)	7.9	9.1	6.8	27.6
δ^2H (‰ VSMOW)	−12.1	−12.4	−12.7	−8.9
$\delta^{18}O$ (‰ VSMOW)	−3.2	−3.1	−3.5	−2.7

HESSD
12, 975–1015, 2015

Table 3. Rainfall–runoff relationships observed during wet season 2013–2014 for Kaap catchment at outlet (X2H022 stream gauge) and average precipitation from Roffiekultuur, Nelshoogte Bos, Satico, and Josefdal Boarder rain stations.

		Event 1	Event 2	Event 3	Event 4
Runoff	Peak flow time and date	13 Dec 13 18:24	30 Dec 13 06:12	16 Jan 14 03:48	31 Jan 14 17:00
	Maximum river depth (m)	2.0	1.0	0.5	0.5
	Peak flow ($m^3 s^{-1}$)	124.0	27.6	6.5	7.1
	Runoff Volume (mm)	3.2	2.6	0.1	0.4
	Time to peak after rainfall started (h)	24.4	31.2	60.8	22.0
Rainfall	Rain start date and time	12 Dec 13 18:00	28 Dec 13 23:00	13 Jan 14 15:00	30 Jan 14 19:00
	Rain duration (h)	7	39	7	26
	Rain depth (mm)	24	78	17	20
	Average rain intensity ($mm h^{-1}$)	3.4	2.0	2.5	0.8
	Maximum rain intensity ($mm h^{-1}$)	9.8	12	5	10
	Antecedent Precipitation Index API_{-7} (mm)	38.7	1.3	7.8	24.9
	API_{-14} (mm)	118.1	12.8	20.0	67.9
	API_{-30} (mm)	390.2	220.8	192.4	223.8

HESSD
12, 975–1015, 2015

Table 4. Percentages of direct runoff [DR] and groundwater [GW] contributions and 70 % uncertainty percentages [W] from 2-component hydrograph separations for wet season 2013–2014 Kaap catchment, South Africa.

Tracer	Event 1			Event 2			Event 3			Event 4		
	DR	GW	W	DR	GW	W	DR	GW	W	DR	GW	W
EC	22	78	6.8	5	95	7.9	6	94	7.0	27	73	4.2
SiO_2	21	79	2.6	6	94	2.5	12	88	2.2	21	79	2.6
$CaCO_3$	29	71	6.3	9	91	6.9	6	94	6.8	24	76	4.6
Mg	22	78	5.6	13	87	6.0	8	92	5.3	24	76	4.0
^{18}O	23	77	8.6	8	92	3.3	10	90	3.1	36	64	12.4
^{2}H	19	81	5.6	5	95	15.0	2	98	19.4	21	79	24.9

HESSD
12, 975–1015, 2015

Table 5. Direct runoff [DR], shallow groundwater [SGW], and deep groundwater [DGW] contributions in (%) and 70 % uncertainty of 3-component hydrograph separations in (%).

Tracers	Event 1			Event 2			Event 3			Event 4		
	DR	SGW	DWG	DR	SGW	DWG	DR	SGW	DWG	DR	SGW	DWG
K and ^{18}O	28	45	26	7	19	74	16	6	78	41	21	37
70 % uncertainty (%)	7.2	5.3	5.8	7.4	3.2	5.1	5.3	3.0	3.9	7.9	6.2	5.8
K and ^{2}H	22	45	33	14	19	67	11	5	84	37	20	42
70 % uncertainty (%)	4.8	6.6	6.4	3.8	3.9	5.5	3.0	2.8	4.0	6.3	6.2	7.6

HESSD
12, 975–1015, 2015

Table 6. Runoff components found in the Kaap catchment.

Component	Transport mechanism	Geology	EC	Alkalinity	Silicates	Nitrates and Sulphates	δ^2H	δ^{18}O
Direct Runoff – Precipitation (P) – Infiltration excess overland flow (Q_O) – Saturation excess overland flow (Q_S)	Direct precipitation on stream channel, Horton overland flow	–	Low to moderate	Low to moderate	Low	Low to moderate	Very depleted (−30 ‰)	Very depleted (−5 ‰)
Shallow groundwater (GW_S)	Horizontal sub-surface stormflow (piston flow, preferential pathways)	Shallow soils, shale, sandstones, siltstones, quartz, greywacke	High	High	Moderate	High	Enriched −9 ‰	Enriched −2 ‰
Deep groundwater (GW_D)	Vertical and horizontal flow, regional flow lines (preferential pathways)	Weathered granite	Moderate to high	High	High	Low	Very enriched (−2 ‰)	Very enriched (−1 ‰)

HESSD
12, 975–1015, 2015

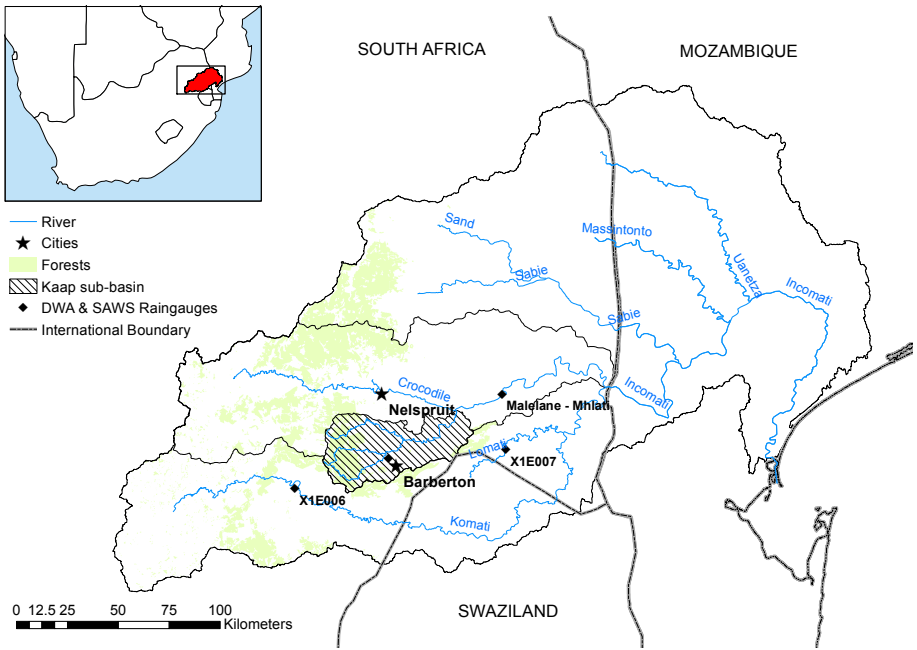

Figure 1. Location of the Kaap catchment in the Incomati basin displaying nearby cities, and DWA and SAWS rain gauges.

HESSD
12, 975–1015, 2015

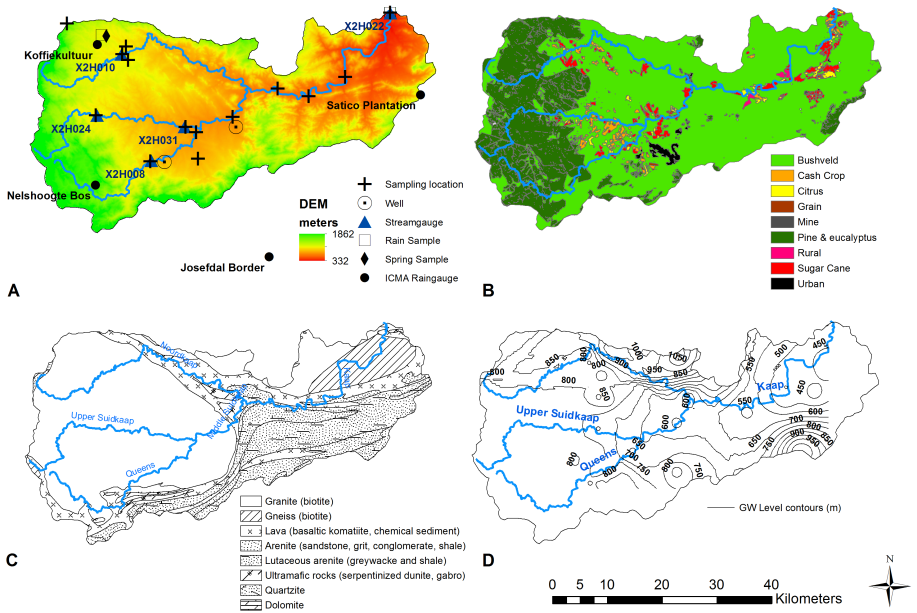

Figure 2. (a) DEM of Kaap catchment with sampling locations and stream and rain gauges locations, **(b)** land use map of Kaap catchment **(c)** geological map, and **(d)** contour map of static groundwater levels (GIS layers are courtesy of Water Research Commission, 2005 South Africa).

HESSD
12, 975–1015, 2015

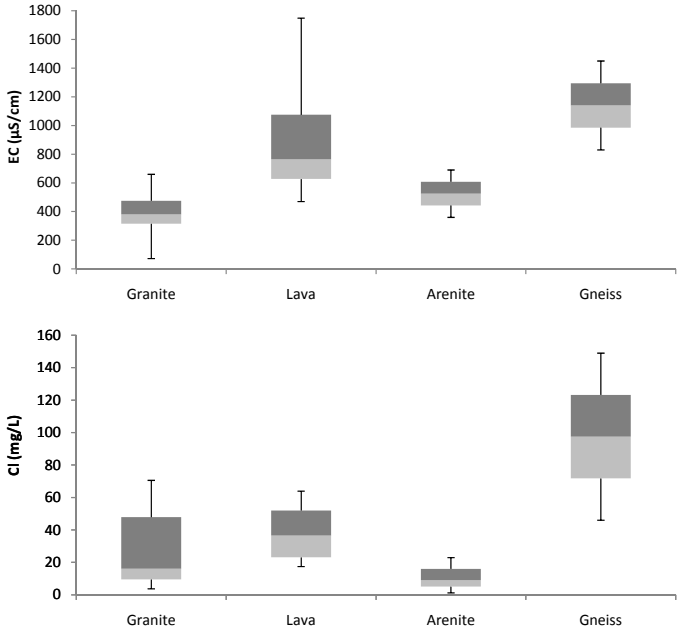

Figure 3. Boxplots of borehole water quality parameters at different geological locations in the Kaap catchment.

HESSD
12, 975–1015, 2015

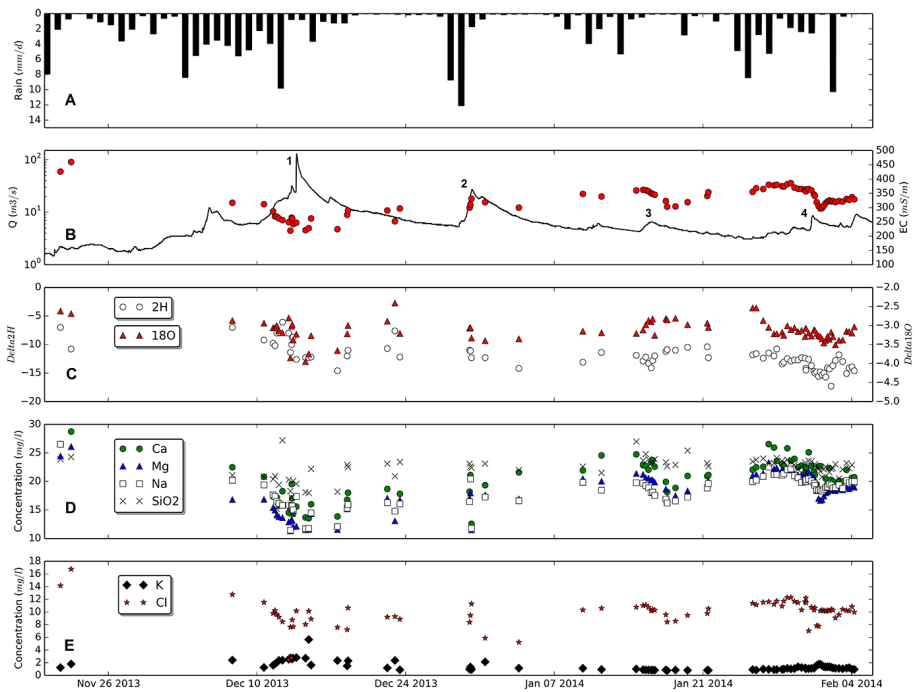

Figure 4. Kaap catchment **(a)** average precipitation in mm d^{-1}, **(b)** discharge at the outlet in m^3 s^{-1} and electrical conductivity µS cm^{-1}, **(c)** delta deuterium and delta oxygen-18 in ‰ VSMOW, **(d)** calcium, magnesium, sodium and silica concentrations at the outlet in mg L^{-1}, and **(e)** chloride and potassium concentrations at the outlet in mg L^{-1}.

HESSD
12, 975–1015, 2015

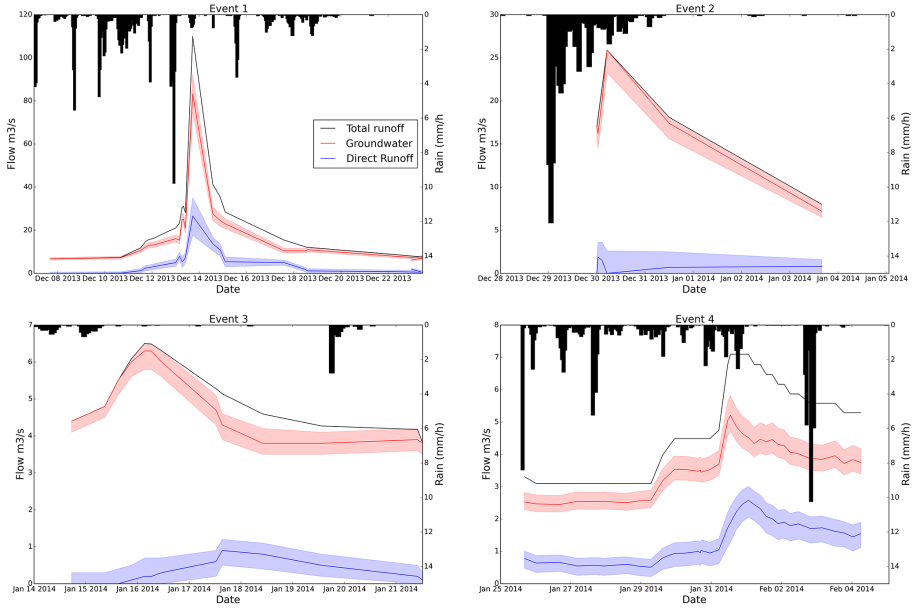

Figure 5. Two component hydrograph separations using electrical conductivity as a tracer. Event 1 and 4 had larger direct runoff contribution coinciding with the total runoff peak. Event 2 and 3 had smaller direct runoff contribution.

HESSD
12, 975–1015, 2015

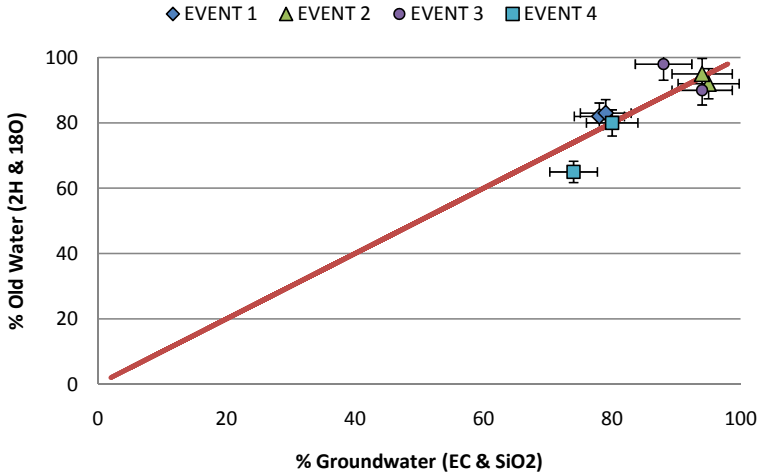

Figure 6. Percentages of groundwater and old water contributions using environmental isotopes (δ^2H and δ^{18}O) and hydrochemical (EC and SiO_2) tracers.

HESSD
12, 975–1015, 2015

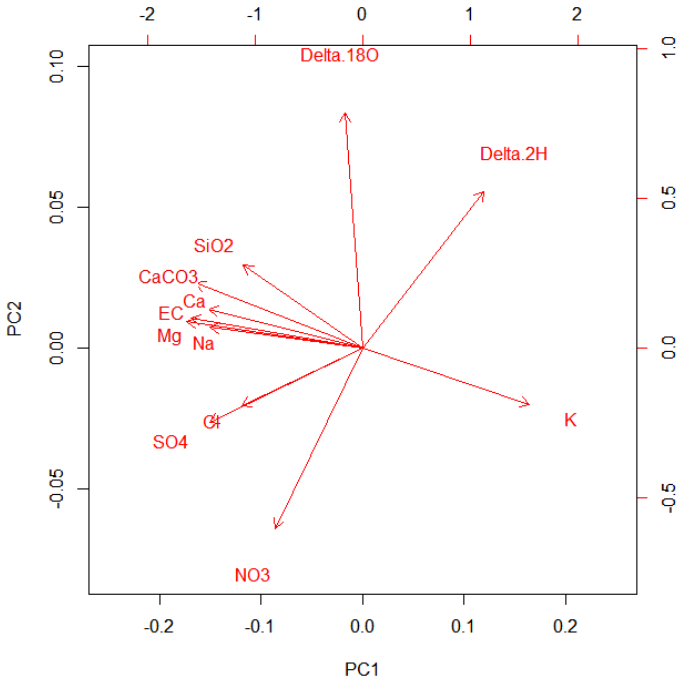

Figure 7. Biplot of principal components generated during PCA analysis of stream water samples using EC, SiO_2, $CaCO_3$, Cl, NO_3-N, SO_4, Na, Mg, K, Ca, δ^2H, $\delta^{18}O$.

HESSD
12, 975–1015, 2015

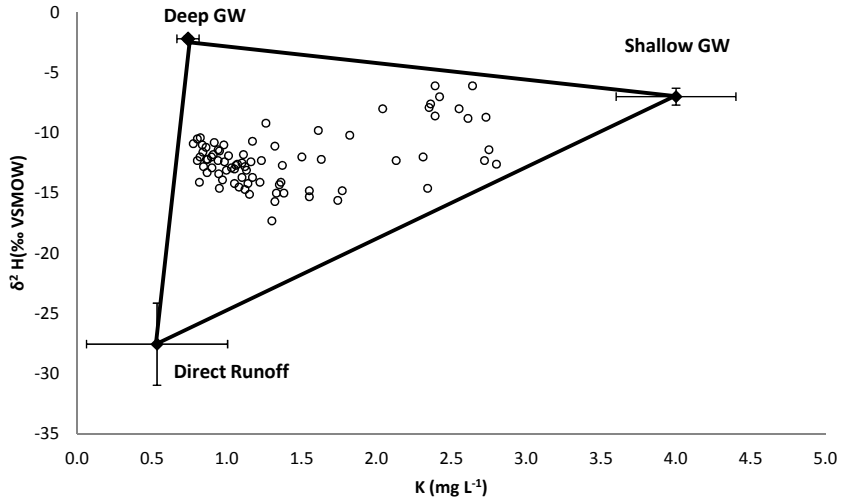

Figure 8. Mixing diagram of δ^2H and K showing stream water samples at outlet for four rain events during wet season 2013–2014.

HESSD
12, 975–1015, 2015

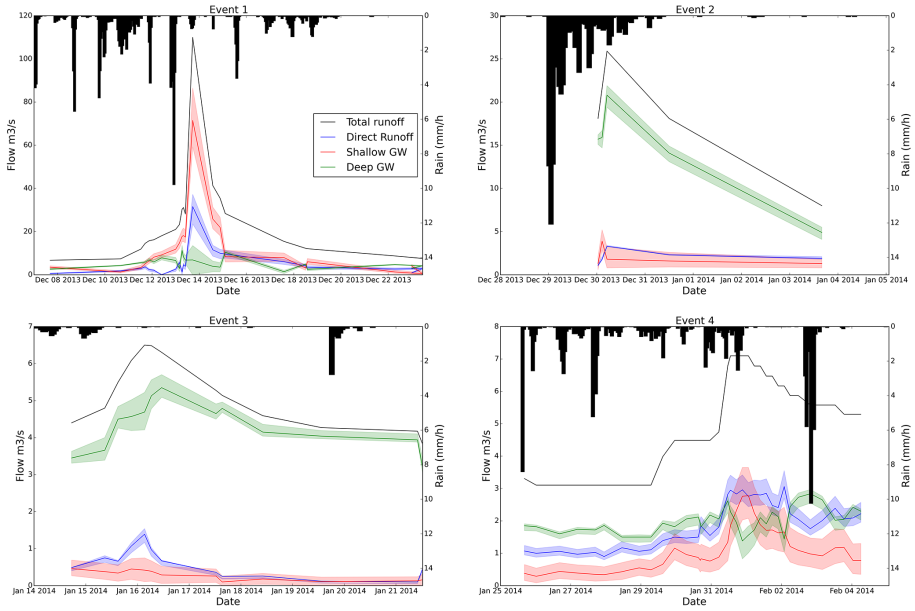

Figure 9. Three-component hydrograph separations using K and ^{2}H.

HESSD
12, 975–1015, 2015

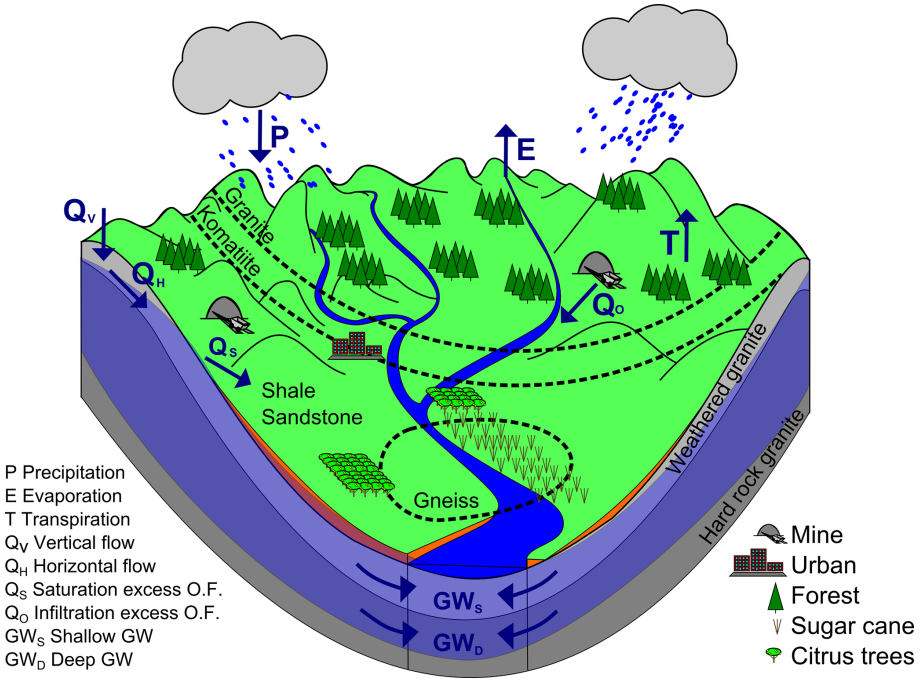

Figure 10. Conceptual diagram of runoff processes in Kaap catchment, South Africa.

HESSD
12, 975–1015, 2015